Available online at www.sciencedirect.com
ScienceDirect
Journal of Power Sources 178 (2008) 758–764
JOURNAL OF POWER SOURCES
www.elsevier.com/locate/jpowsour

Superelastic electrodes using Ti–Ni shape memory alloys

Han-Seong Kim, Joo-Suk Kim, Min-Gyun Kim, Kwon-Koo Cho, Tae-Hyun Nam *

Division of Advanced Materials Engineering, ERI and i-Cube Center, Gyeongsang National University, 900 Gajwa-dong, Jinju, Gyeongnam 660-701, Republic of Korea

Received 30 June 2007; received in revised form 1 August 2007; accepted 2 August 2007
Available online 6 August 2007

Abstract

Ni and Ti sulfides are formed on the surface of a $Ti_{50}Ni_{50}$ alloy by annealing the alloy at 873 K for 0.24–72 ks under the sulfur pressure of 160 kPa, and then microstructures, martensitic transformation behavior, shape memory characteristics, superelasticity and electrochemical properties are investigated by means of scanning electron microscopy, X-ray diffraction, differential scanning calorimetry, thermal cycling tests under constant load and tensile tests. NiS_2 particles are formed first on the surface of the alloy, and then are grown and coalesced with increasing annealing time. When annealing time is longer than 1.2 ks, in addition to NiS_2, $Ti_{8.2}S_{11}$ sulfide is formed, and therefore the surface sulfide layers is consisted of NiS_2 and $Ti_{8.2}S_{11}$. A $Ti_{50}Ni_{50}$ alloy with the surface sulfide layers shows the shape memory effect and superelasticity clearly. A $Ti_{50}Ni_{50}$ alloy with the surface sulfide layers shows clear discharge behavior with an increase of annealing time. Multi-voltage plateaus of 1.89, 1.70 and 1.42 V are observed at a cell with electrode annealed for 1.2 ks and an additional plateau at 2.0 V appeared at cells of 3.6 and 10.8 ks. NiS_2 is not transformed into pure Ni and Li_2S during discharging process directly but is transformed by way of intermediate phases such as NiS and Ni_3S_2.

Keywords: Sulfides cathode; Ti–Ni current collector; Secondary battery; Superelasticity; Discharge behavior

1. Introduction

Secondary batteries are usually consisted of electrodes, electrolyte and current collectors. Al, Cu and stainless steel are currently used as current collectors of secondary battery because of their high-corrosion resistance and low-electrical resistance. Flexible secondary batteries are recognized to be necessary for many portable electrical appliances, such as wearable computer because they are heading for small system and multifunction. In order to obtain a flexible secondary battery, its constituents, i.e., electrodes, electrolyte and current collectors should be flexible.

Metal sulfides such as Co, Cr, Cu, Mn, Ti, V and Ni sulfides have been studied as a cathode material of secondary batteries because of their high-energy density [1,2]. Those electrode materials usually are used as powders and they are pasted on current collectors with polymer-based binders. Liquid and polymer-based materials are usually used as electrolytes.

Electrode materials and electrolytes are not considered to be harmful for the flexibility of secondary batteries because polymer-based materials generally has relatively good flexibility comparing with metallic materials. However, current collector materials such as Al, Cu and stainless steel are considered to be harmful for the flexibility because they have small elastic deformation limit (usually less than 0.2%). Therefore, in order to realize flexible secondary batteries, new current collector materials with large elastic deformation limit. Also current collector materials are required to have high-corrosion resistance and low-electrical resistivity.

A feasibility study to apply Ti–Ni alloys for current collector materials of secondary batteries [3] was made, because they shows the superelasticity originated from the thermo-elastic martensitic transformation [4]. Three kinds of thermo-elastic martensitic transformation occurs in Ti–Ni-based alloys, i.e., the B2(cubic)-R(trigonal) [5–7], B2-B19(orthorhombic) [8,9], B2-B19′(monoclinic) transformations [10]. Among them, the B2-B19′ transformation is considered to be suitable for battery application because it has the largest superelastic strain (∼7%). Also many researches have been made for improving the superelasticity of Ti–Ni alloys [11–13]. According to the previous study [3], Ti–Ni alloy is a very suitable for current col-

* Corresponding author. Tel.: +82 55 751 5307; fax: +82 55 759 1745.
E-mail address: tahynam@gsnu.ac.kr (T.-H. Nam).

0378-7753/$ – see front matter © 2007 Elsevier B.V. All rights reserved.
doi:10.1016/j.jpowsour.2007.08.003

lector material of flexible secondary batteries in a Li/S battery considering the superelasticity, good-corrosion resistance and relatively low-electrical resistivity.

Recently, there were attempts to fabricate metal sulfides layers such as Ni sulfides and Ti sulfides on Ti–Ni alloy current collectors by annealing Ti–Ni alloys under sulfur atmosphere [14,15]. Ni and Ti sulfides acted as a cathode and Ti–Ni alloys acted as a current collector in the novel electrode/current collector system. The sulfide/ Ti–Ni alloy system showed the superelasticity clearly [15]. Furthermore, even after 3% deformation, the sulfide layers were not detached from the Ti–Ni current collector [15]. The battery exhibited a clear charge–discharge behavior [14]. Therefore, it was concluded that the novel sulfides/Ti–Ni alloys system were available for realizing a flexible secondary battery. However, effects of annealing condition on microstructures and electrochemical properties of the novel sulfides/Ti–Ni alloys system are not studied yet. In the present study, therefore, sulfides/Ti–Ni alloy systems were prepared at various annealing times, and then their microstructures, martensitic transformation behavior, shape memory effect, superelasticity and electrochemical properties were investigated.

2. Experimental procedure

A $Ti_{50}Ni_{50}$ alloy ingot was prepared by vacuum induction melting and then hot rolled into a sheet. After hot rolling, the sheet was cold rolled with a final cold working ratio of 35%. All specimens cut from the cold rolled sheet were annealed at 673 K for 3.6 ks in vacuum. Before using the specimens as substrates, they were mechanically polished in order to remove oxide films, and then they were cleaned using acetone and methyl alcohol. After cleaning, they were put into a silica tube of 15 mm diameter with sulfur and then sealed in vacuum. The vacuum sealed ampoules were isothermally annealed at 873 K for 0.24–72 ks. The sulfur pressure inside the ampoules was 160 kPa.

Microstructure of specimens was observed using scanning electron microscope (SEM). In order to investigate the crystal structure of sulfides, X-ray diffraction (XRD) experiments were made using Cu Kα radiation with a scanning rate of $2^\circ\,min^{-1}$. Transformation behavior of specimens was investigated by differential scanning calorimetry (DSC) measurements with a cooling and heating rate of $0.17\,K\,s^{-1}$. The shape memory characteristics were investigated by thermal cycling tests under constant load with a cooling and heating rate of $0.017\,K\,s^{-1}$. Elongation on cooling and its recovery on heating were measured by linear variable differential transformer. The superelasticity was examined by tensile tests at various temperatures with a strain rate of $10^{-4}\,s^{-1}$.

For investigating electrochemical properties, Li foil was used as an anode and sulfides formed on a $Ti_{50}Ni_{50}$ alloy were used as a cathode. A $Ti_{50}Ni_{50}$ alloy was used as a current collector and 1 M $LiCF_3SO_3$ in tetraethylenglycol dimethylether (TEGDME) was used as an electrolyte. Li/sulfides cells were assembled in stainless steel cell holders, and then discharged galvanostatically. The rest time before discharging was 4 h, where open circuit voltage (OCV) was stabilized for cells. The current density was 20, 30 and 60 $\mu A\,cm^{-2}$ for cells with electrodes annealed for 1.2, 1.6 and 3.6 ks, respectively. Mass of active materials was calculated from density (NiS_2: $4.00\,g\,cm^{-1}$, $Ti_{8.2}S_{11}$: $3.59\,g\,cm^{-1}$) and thickness of films measured from SEM images.

3. Results and discussion

3.1. Microstructures and transformation behavior

Fig. 1 shows SEM micrographs of surface of specimens annealed at 873 K for various times under the sulfur pressure of 160 kPa. For comparison, a micrograph of the specimen annealed at 873 K without sulfur is shown in Fig. 1(a). Comparing Fig. 1(a) and (b), it is found clearly that small particles

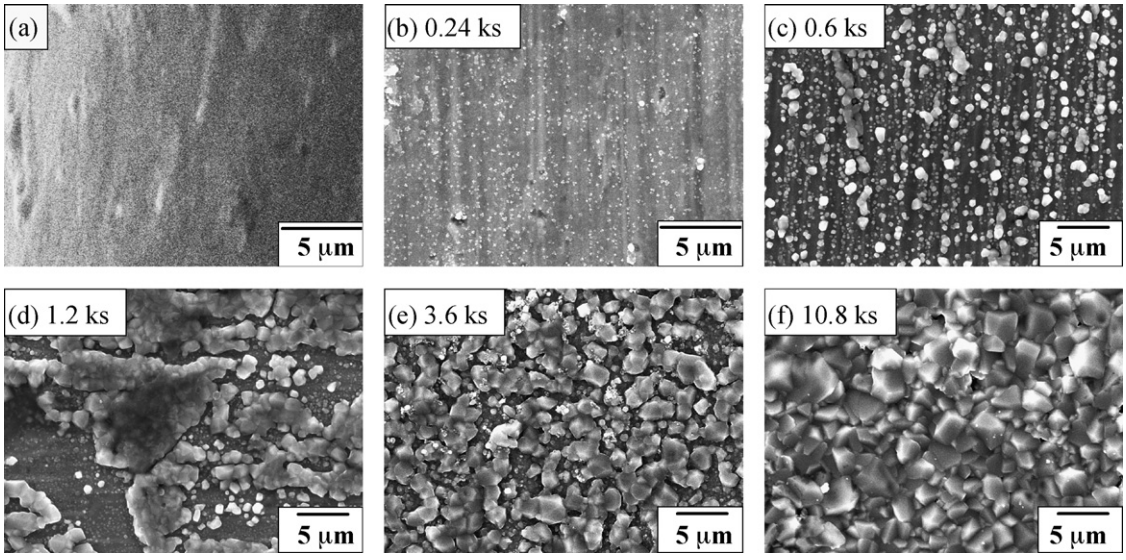

Fig. 1. SEM micrographs of surface of specimens annealed under sulfur atmosphere. Annealing times are indicated in each micrograph: (a) was obtained from the specimen annealed without sulfur.

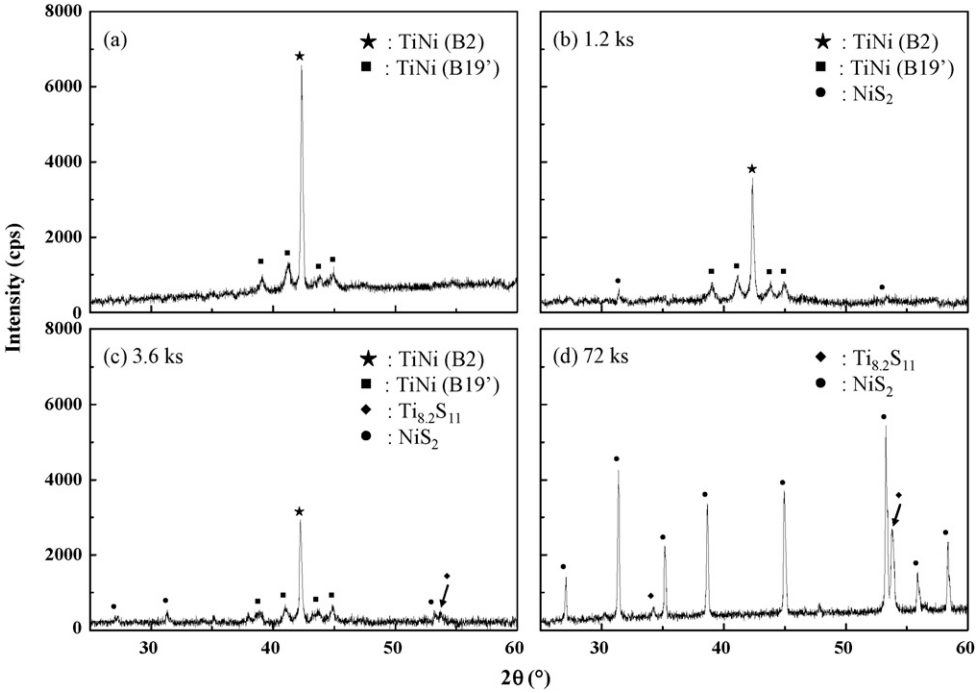

Fig. 2. X-ray diffraction patterns of specimens annealed under sulfur atmosphere. Annealing times are indicated in each pattern: (a) was obtained from the specimen annealed without sulfur.

are formed by annealing for 0.24 ks under sulfur atmosphere. It is also found that particles grow with increasing annealing time, and then are coalesced each other. In order to characterize the particles in Fig. 1, XRD experiments were made on the specimens. Fig. 2 shows typical XRD patterns obtained. For comparison, a XRD pattern of the specimen annealed at 873 K without sulfur is shown in Fig. 2(a). Diffraction peaks corresponding to the B2 parent phase and the B19′ martensite are observed in Fig. 2(a). In the pattern of Fig. 2(b) obtained from the specimen annealed for 1.2 ks under sulfur atmosphere, in addition to the peaks of the B2 parent phase and the B19′ martensite, those corresponding to NiS_2 are found. Therefore, the particles observed in Fig. 1(d) are known to be NiS_2.

Comparing Fig. 2(a) and (b), it is found that intensity of the peak of the B2 parent phase decreases, while relative intensity of diffraction peak of the B19′ martensite to the B2 parent phase decreases by annealing the specimen under sulfur atmosphere. This is related with the fact that NiS_2 particles are formed on the surface of a $Ti_{50}Ni_{50}$ alloy, resulting in a decrease in Ni content near the surface of the alloy. The B2-B19′ martensitic transformation start temperature (Ms) is known to increase with decreasing Ni content, and thus volume fraction of the B19′ martensite increases [16]. From Fig. 2(a) and (b), it is concluded that NiS_2 is formed on the surface of a $Ti_{50}Ni_{50}$ alloy by annealing under sulfur atmosphere. With prolonging annealing time up to 3.6 ks, in addition to NiS_2, $Ti_{8.2}S_{11}$ appears as shown in Fig. 2(c) where diffraction peaks of the B2, B19′, NiS_2 and $Ti_{8.2}S_{11}$ are observed simultaneously. Further increasing annealing time, intensity of diffraction peaks of NiS_2 and $Ti_{8.2}S_{11}$ increases, while diffraction peaks of the B2 and B19′ disappear as seen in Fig. 2(d). Therefore, it is concluded that reaction products formed on the surface of a $Ti_{50}Ni_{50}$ alloy in Fig. 1(e) and (f) are a mixture of NiS_2 and $Ti_{8.2}S_{11}$ sulfides.

Fig. 3 is a micrograph showing cross section of the specimen annealed for 72 ks under sulfur atmosphere. It is found that the surface layer formed on the surface of a $Ti_{50}Ni_{50}$ alloy is consisted with two distinct layers. The outer layer is found to be dense, while the inner layer is porous. Thickness of the outer layer and inner layer is found to be about 10 and 23 μm, respectively. In order to characterize the surface layer, XRD experiments were made on specimen with successively removing the surface layer, and then XRD patterns obtained are shown in Fig. 4. Before removing the surface layer, diffraction

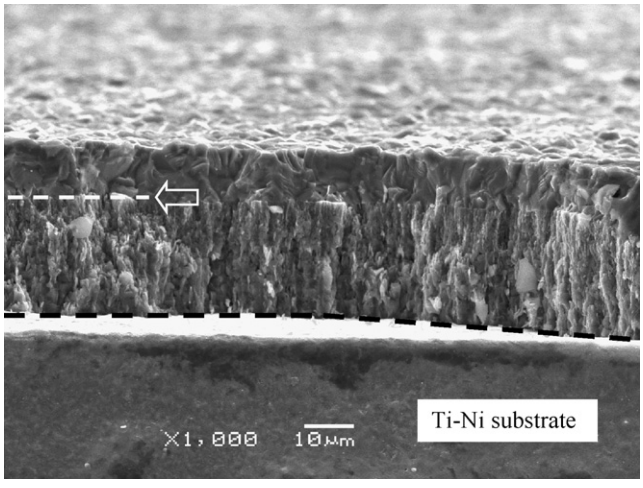

Fig. 3. A micrograph showing cross section of the specimen annealed for 72 ks under sulfur atmosphere.

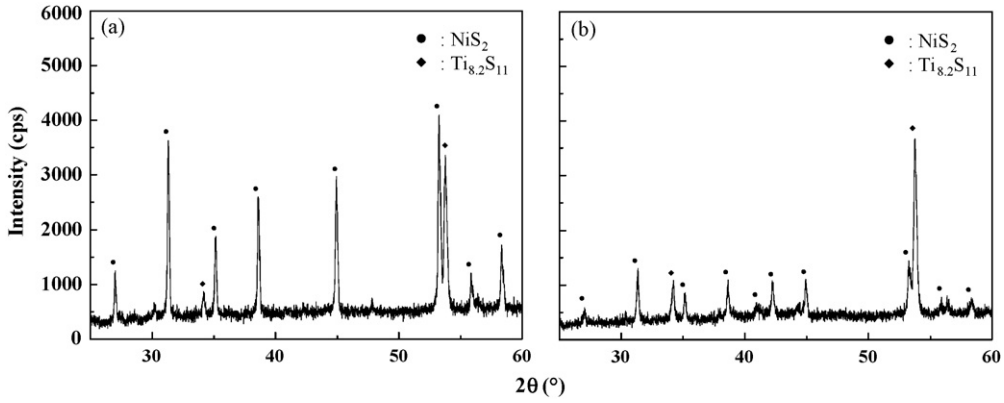

Fig. 4. X-ray diffraction patterns obtained with successively removing the surface layer of the specimen annealed for 72 ks under sulfur atmosphere.

peaks corresponding to NiS_2 and $Ti_{8.2}S_{11}$ sulfide were observed as shown in Fig. 2(d). Fig. 4(a) is a XRD pattern obtained after removing the outer layer. Diffraction peaks corresponding to NiS_2 and $Ti_{8.2}S_{11}$ sulfide appear. Comparing Fig. 2(d) and Fig. 4(a), it is found that intensity of the diffraction peaks of NiS_2 decreases, while that of $Ti_{8.2}S_{11}$ increases by removing the outer layer. Fig. 4(b) is a XRD pattern obtained after removing the surface layer by about 30 μm. Diffraction peaks corresponding to the B2 parent phase, NiS_2 and $Ti_{8.2}S_{11}$ sulfides appear. Diffraction peak of the B2 parent phase appears because the surface layer remained is only about 3 μm, and thus scattering occurs at the substrate (Ti-50.0 alloy) also. Comparing Fig. 4(a) and (b), it is clear that intensity of diffraction peaks of $Ti_{8.2}S_{11}$ increases, while that of NiS_2 decreases with removing the surface layer more and more. Therefore, it is considered that the outer layer is mainly NiS_2 and inner layer is mainly $Ti_{8.2}S_{11}$. Similar result was obtained from the specimen annealed at 873 K for 72 ks under the sulfur pressure of 80 kPa [14]. From Figs. 2 and 4, it is concluded that NiS_2 is formed first, and then $Ti_{8.2}S_{11}$ is formed on the surface of the substrate by annealing under sulfur atmosphere. From the previous study [17], it has been known that Ti sulfide is more stable than Ni sulfide. However, in the present study, Ni sulfide was formed earlier than Ti sulfide. This may be attributed to Ti oxides formed on the surface of a $Ti_{50}Ni_{50}$ alloy, which suppresses a reaction between Ti and S. In Fig. 2, however, any diffraction peaks corresponding to Ti oxides are not observed. This is possibly ascribed to that Ti oxides are very thin and/or amorphous.

DSC curves of the specimens annealed under sulfur atmosphere are shown in Fig. 5. For comparison, the specimen annealed without sulfur is shown also in Fig. 5(a). Annealing

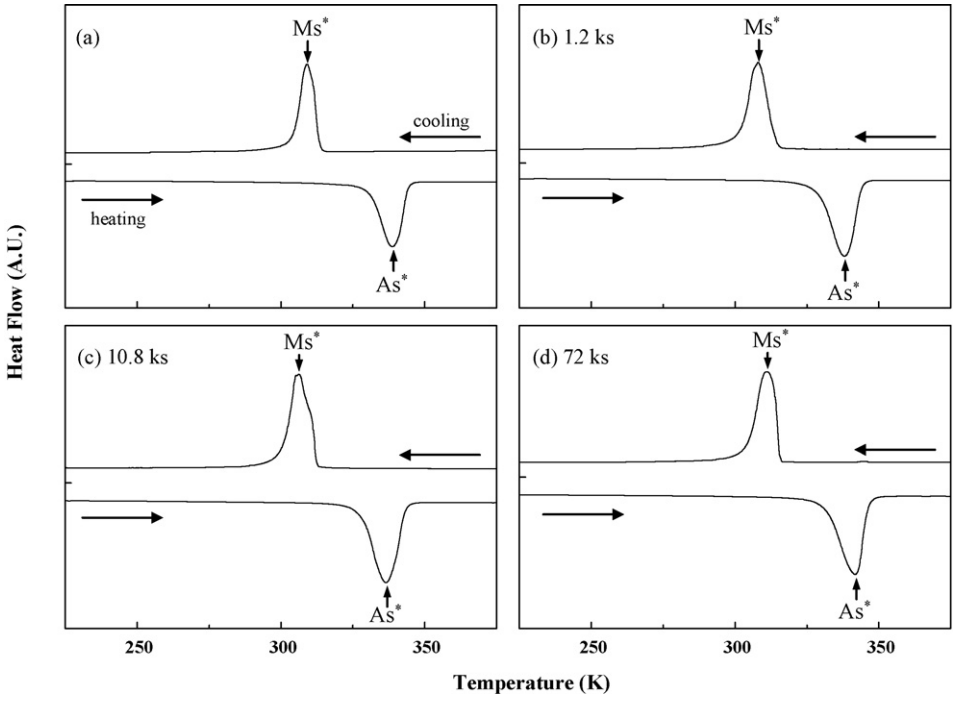

Fig. 5. DSC curves of the specimens annealed under sulfur atmosphere. Annealing times are indicated in each curve: (a) was obtained from the specimen annealed without sulfur.

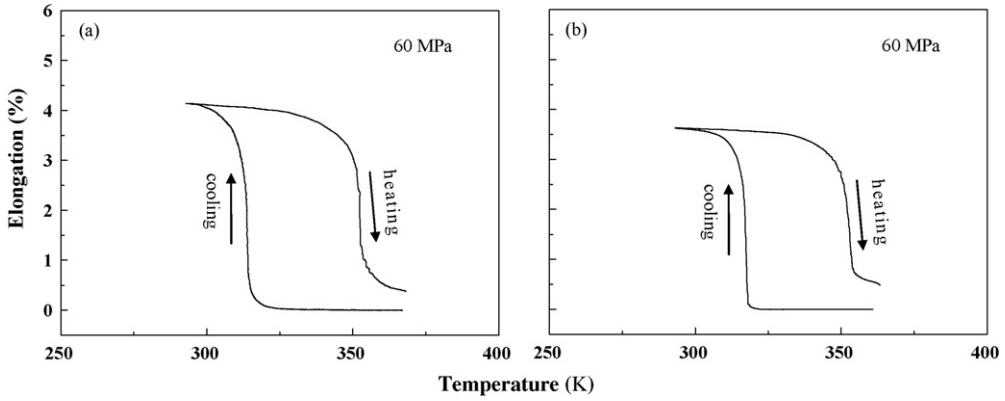

Fig. 6. Elongation vs. temperature curves of specimens: (a) annealed without sulfur and (b) annealed under sulfur atmosphere for 72 ks.

time is indicated in each curve. Clear DSC peaks are observed on each cooling and heating curve in all specimens. In general, Ti–Ni alloys annealed at 873 K after cold working show B2-B19′ transformation [11]. Therefore, the DSC peaks in Fig. 5 are ascribed to the B2-B19′ transformation. Comparing the curves, any significant changes in shape and position of the peaks are not found by annealing under sulfur atmosphere. Therefore, it is concluded that annealing under sulfur atmosphere does not affect transformation behavior and transformation temperatures of a $Ti_{50}Ni_{50}$ alloy significantly.

3.2. Shape memory effect and superelasticity

In order to investigate the shape memory effect, thermal cycling tests were made on the specimen annealed for 72 ks under sulfur atmosphere at 60 MPa, and then elongation versus temperature curve obtained is shown in Fig. 6(b). For comparison, the curve of the specimen annealed for 3.6 ks without sulfur is shown also in Fig. 6(a). Elongation occurred at Ms on cooling is ascribed to the B2-B19′ transformation in both specimens. It is clear that the elongation occurred on cooling is recovered partly on heating and a residual elongation which was not recovered on heating is observed in both specimens. The residual elongation is due to a plastic deformation occurred on thermal cycling. It is also found that the elongation associated with the B2-B19′ transformation of the curve of (b) is smaller than that of the curve of (a). Since the sulfide layer formed on the surface of a $Ti_{50}Ni_{50}$ alloy does not undergo martensitic transformation, it would not show the elongation associated with the transformation.

Fig. 7(b) shows a stress–strain curve off the specimen annealed for 72 ks under sulfur atmosphere. For comparison, the curve of the specimen annealed for 3.6 ks without sulfur is shown also in Fig. 7(a). In loading curve, a stress plateau is observed where a strain increases without increasing stress significantly after an elastic deformation. The strain developed at the stress plateau is associated with the stress-induced B2-B19′ transformation. In unloading curve, the strain developed on loading is recovered by unloading. It is noted that the strain is not recovered completely on unloading in Fig. 7(a), i.e., partial superelasticity. This is ascribed to the fact that annealing was made at 873 K after cold working which is too high for obtaining perfect superelasticity [11]. The superelastic recovery ratio defined as (A/B) × 100 (%) is measured to be 77%. In Fig. 7(b), the superelastic recovery ration is known to be 67%, which is smaller than Fig. 7(a). This is attributed to the sulfide layer which suppresses the superelastic recovery of a $Ti_{50}Ni_{50}$ alloy.

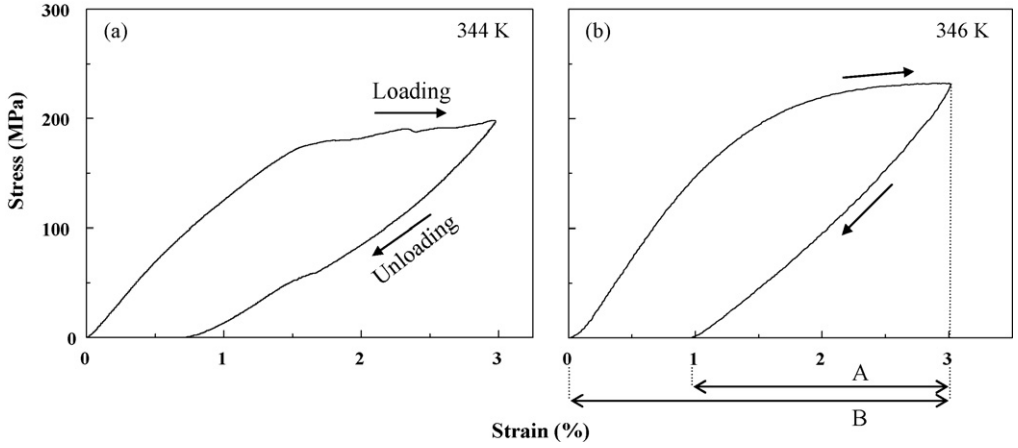

Fig. 7. Stress vs. strain curves of specimens: (a) annealed without sulfur and (b) annealed under sulfur atmosphere for 72 ks. All curves were obtained at A_f (the reverse transformation finish temperature).

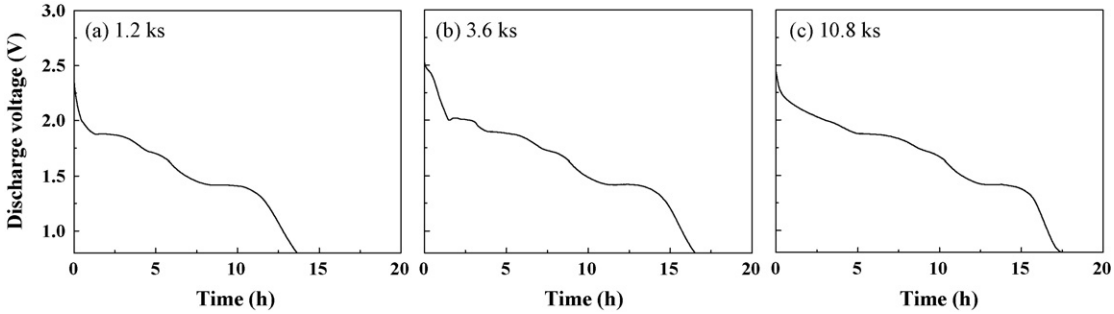

Fig. 8. Discharge curves of specimens annealed under sulfur atmosphere. Annealing times are indicated in each curve.

3.3. Discharge characteristics

Fig. 8 shows galvanostatic discharge curves of cells with the specimens (electrodes) annealed for 1.2, 3.6 and 10.8 ks, respectively, under sulfur atmosphere. From X-ray diffractions, sulfide layers formed on the surface of a $Ti_{50}Ni_{50}$ alloy were found to be a mixture of NiS_2 and $Ti_{8.2}S_{11}$.

All electrodes show clear discharge behavior with multi-voltage plateaus, depending on annealing time. Multi-voltage plateaus are observed at 1.89, 1.70 and 1.42 V in the cell with the electrode annealed for 1.2 ks where only NiS_2 exists on the Ti–Ni alloy. Assuming that the total discharging reaction of NiS_2 is as follows:

$$NiS_2 + 2Li \rightarrow NiS + Li_2S \quad (1)$$

$$3NiS + 2Li \rightarrow Ni_3S_2 + Li_2S \quad (2)$$

$$Ni_3S_2 + 4Li \rightarrow 3Ni + 2Li_2S \quad (3)$$

The voltage plateaus at 1.89, 1.70 and 1.42 V are ascribed to reactions (1)–(3), respectively. The overall reaction can be summarized as follows:

$$NiS_2 + 4Li \rightarrow Ni + 2Li_2S \quad (4)$$

The reaction (4) occurs at 1.95 V. In the discharge curves, voltage plateau corresponding to 1.95 V is not observed. This suggests that NiS_2 is not transformed into pure Ni and Li_2S directly during discharging process. NiS_2 is considered to be dissociated by forming NiS, and then NiS is dissociated by forming Ni_3S_2 and finally NiS_2 is transformed into pure Ni and Li_2S during discharging process. More detail investigation on intermediate products is in progress.

For electrodes annealed for 3.6 and 10.8 ks, a fresh plateau together with the plateaus of 1.2 ks is found at 2.0 V. The appearance of 2.0 V plateau would be associated with a reaction of $Ti_{8.2}S_{11}$ and Li. This can be explained with the facts that the formation of $Ti_{8.2}S_{11}$ phase begins to occur at electrode annealed for 3.6 ks as shown in Fig. 2, and the 2.0 V plateau is sloped with increasing annealing time up to 10.8 ks. It is directly related to the morphological change of electrode surfaces. In the electrode annealed for 3.6 ks, although the $Ti_{8.2}S_{11}$ layer is formed below the NiS layer, electrolyte can reach to the $Ti_{8.2}S_{11}$ layer through many pore channels (Fig. 1(e)) and lead to a stable discharge reaction. On the other hand, in the electrode annealed for 10.8 ks, a film-like NiS_2 layer is formed on the $Ti_{8.2}S_{11}$ layer (Fig. 1(f)), which delays the inflow of electrolyte into the $Ti_{8.2}S_{11}$ layer and subsequently leads to an unstable reaction. Thus, it is concluded that discharge behavior over 2 V is closely related to the presence of $Ti_{8.2}S_{11}$.

Discharge times of cells with electrodes annealed for 1.2, 3.6 and 10.8 ks are 13.5, 16.3 and 17.5 h, respectively. The discharge time at each voltage plateaus is constantly kept except 2.0 V plateau, indicating that specific capacity of NiS_2 is nearly the same for all cells. However, the discharge time over 2.0 V plateau increases from 3.5 to 5 h, indicating that specific capacity of $Ti_{8.2}S_{11}$ increase with increasing annealing time. The change of capacity is considered to be associated with difference in resistance of cells, depending on surface morphology of electrodes. Open circuit voltages (OCVs) of cells with the electrodes annealed for 1.2, 3.6 and 10.8 ks are 2.64, 2.83 and 3.01 V, respectively. Despite of an increase in layer thickness, OCV increases with prolonging annealing time. This suggests that the electrode annealed for 3.6 ks with discontinuous sulfide layer has high-surface area, which increases resistance of the cell, while electron transfer easily occurs at continuous sulfide surface of 10.8 ks, which decreases resistance of cell and increases the specific capacity of $Ti_{8.2}S_{11}$.

4. Conclusions

Ni and Ti sulfides were formed on the surface of a $Ti_{50}Ni_{50}$ alloy by annealing the alloy at 873 K for 0.24–72 ks under the sulfur pressure of 160 kPa, and then microstructures, martensitic transformation behavior, shape memory characteristics, superelasticity and electrochemical properties were investigated. Results obtained are as follows:

(1) NiS_2 particles were formed by annealing for 0.24 ks under sulfur atmosphere, and then were grown and coalesced with increasing annealing time. When annealing time was longer than 3.6 ks, in addition to NiS_2, $Ti_{8.2}S_{11}$ sulfide was formed. The surface sulfide layer was consisted of two distinct layers where the outer layer was mainly NiS_2 and the inner layer was mainly $Ti_{8.2}S_{11}$.
(2) A $Ti_{50}Ni_{50}$ alloy annealed under sulfur atmosphere showed very similar transformation behavior (B2-B19′ transformation) and temperatures to those of the alloy annealed without sulfur.

(3) A $Ti_{50}Ni_{50}$ alloy with surface sulfide layer with a thickness of 33 μm showed the shape memory effect and superelasticity clearly.
(4) A $Ti_{50}Ni_{50}$ alloy annealed under sulfur atmosphere showed clear discharge behavior with annealing time. Multi-voltage plateaus at 1.89, 1.70 and 1.42 V were observed at a cell with electrode annealed for 1.2 ks where only NiS_2 phase exists on the Ti–Ni alloy. The multi-voltage plateaus suggested that NiS_2 was not transformed into pure Ni and Li_2S during discharging process but was transformed by way of intermediate phase such as NiS and Ni_3S_2. An additional plateau at 2.0 V with the presence of $Ti_{8.2}S_{11}$ was observed in discharge curves of 3.6 and 10.8 ks.

Acknowledgement

This work was supported by University IT Research Center Project in Gyeongsang National University.

References

[1] E. Peled, D. Golodnitsky, E. Strauss, J. Lang, Y. Lavi, Electrochem. Acta 43 (1998) 1593.
[2] R.A.J. Sharma, Electrochem. Soc. 123 (1976) 448.
[3] G.B. Cho, S.M. Park, S.S. Jeong, K.W. Kim, T.H. Nam, Mater. Lett. 60 (2006) 643.
[4] W.J. Buehler, J.W. Gilfrich, R.C. Wiley, J. Appl. Phys. 34 (1963) 1473.
[5] M. Matsumoto, T. Honma, Proceedings Of the First Japan Institute of Metals International Symposium on Martensite, JIM, Kobe, 1976, p. 199.
[6] C.M. Hwang, C.M. Wayman, Metall. Trans. 15A (1984) 1155.
[7] V.N. Khachin, Y.I. Paskal, V.E.A.A. Gjunter, Monasevich, V.P. Sivokha, Phys. Met. Metall. 46 (1978) 49.
[8] Y. Shugo, H. Hasegawa, T. Honma, Bull. Res. Inst. Mineral Dress. Metall. Tohoku Univ. 37 (1981) 79.
[9] T. Tadaki, C.M. Wayman, Metallography 15 (1982) 233.
[10] Y. Kudoh, M. Tokonami, S. Miyazaki, K. Otsuka, Acta Metall. 33 (1985) 2049.
[11] S. Miyazaki, Y. Ohmi, K. Otsuka, Y. Suzuki, J. de Phys. 43 (Suppl.) (1982) C4–C255.
[12] M. Nishida, T. Honma, J. de Phys. 43 (Suppl.) (1982) C4–C75.
[13] T. Saburi, T. Tatsumi, S. Nenno, J. de Phys. 43 (Suppl.) (1982) C4–C261.
[14] T.H. Nam, S.M. Park, K.K. Cho, Mater. Sci. Forum 486–487 (2005) 622.
[15] G.B. Cho, K.W. Kim, H.J. Ahn, K.K. Cho, T.H. Nam, J. Alloy Compd., in press.
[16] R.J. Wasilewski, S.R. Butler, J.E. Hanlon, D. Worden, Metall. Trans. A. 2 (1971) 229.
[17] S.R. Shatynski, Oxid. Met. 11 (1977) 307.